

Strand breakage detection in prestressed multi-strand anchorage structures using PZT interface technique

Chẩn đoán sự hư hỏng tao cáp dự ứng lực trong vùng neo cáp sử dụng hiệu trở kháng

Phan Ngoc Tuong Vy, Dang Ngoc Loi*
Phan Ngọc Tường Vy, Đặng Ngọc Lợi*

Urban Infrastructure Faculty, Mien Tay Construction University, Vinh Long City, Vietnam
Khoa Kỹ thuật Hạ tầng - Đô thị, Trường Đại học Xây dựng Miền Tây, Vĩnh Long, Việt Nam

(Ngày nhận bài: 29/11/2022, ngày phản biện xong: 22/12/2022, ngày chấp nhận đăng: 15/01/2023)

Abstract

In this paper, the implementation of the PZT interface technique for monitoring strand breakage in a prestressed concrete anchorage zone is presented. First, the fundamental of the PZT interface for impedance monitoring is briefly reviewed. Second, a FE (finite element) analysis of a multi-strand concrete anchorage equipped with an array of PZT interfaces is analyzed to obtain impedance signatures under a series of strand breakage events. Last, variations in impedance responses of the PZT array are quantified using root-mean-square-deviation (RMSD), and the linear tomography analysis of impedance's RMSD indices is utilized to localize damage strands. The result reveals that locations of single and double outer damaged strands are successfully identified, but the location of a center damage strand is not clearly determined in multiple damage cases.

Keywords: Strand breakage; damage detection; anchorage zone; impedance technique.

Tóm tắt

Trong bài báo này, ứng dụng của kỹ thuật đo trở kháng từ PZT sensor thông qua tầm tiếp xúc để xác định hư hỏng tao cáp trong vùng neo cáp bê tông dự ứng lực được trình bày. Trước tiên, nền tảng cơ bản của việc sử dụng tín hiệu trở kháng cho việc quan trắc kết cấu công trình được tóm tắt. Tiếp theo, mô hình phần tử hữu hạn của vùng neo cáp với nhóm PZT sensor được phân tích để thu tín hiệu trở kháng của PZT sensor dưới sự mất mát lực dự ứng lực của các tao cáp. Sau đó, sự thay đổi trong tín hiệu trở kháng của PZT sensor được xác định thông qua chỉ số RMSD, và các chỉ số RMSD của PZT sensor được sử dụng để xác định vị trí tao cáp hư hỏng. Kết quả nghiên cứu chỉ ra rằng trường hư hỏng của tao cáp biên được phát hiện thành công, nhưng sự hư hỏng của tao cáp giữa thì không được xác định rõ ràng trong trường hợp hư hỏng nhiều tao cáp.

Từ khóa: Hư hỏng tao cáp; chẩn đoán công trình; vùng neo cáp, tín hiệu trở kháng.

*Corresponding Author: Dang Ngoc Loi, Urban Infrastructure Faculty, Mien Tay Construction University, Vinh Long City, Vietnam;

Email: dangngocloi@mtu.edu.vn

1. Introduction

In recent years, a number of tendon-anchorage failures in post-tensioning bridges in the US have been reported [1-3]. Bridges have been evaluated based on the structural performances with a grade scale of A to F, which was excellent to unacceptable conditions. It was estimated that it needs 123 billion dollars to retrofit bridges graded as low as D+ and C. Furthermore, for a newly built PSC (prestressed concrete) beam, it shows that stressing force loss was about 8% in the first seven years [4] after construction. It is known that once prestress force loss reaches a threshold, it could lead to cracks or excessive deflections in concrete components. Due to its critical role, the prestress force should be accurately observed to guarantee structural safe and avoid structural failures (e.g., Genoa Bridge in 2018 [5]).

Various structural health monitoring methods have been proposed for monitoring the health condition of PSC structures [6-8]. Among those, impedance-based methods have been utilized to detect the prestress-loss in PSC structures [9-12]. For the cost-effective technique, electromechanical impedance responses of the anchorage zone are acquired from low-cost PZT (lead zirconate titanate) patches, and the EM impedance variations are quantified and utilized as a prestress-loss indicator. The methods have been widely studied for the health monitoring of various civil structures (e.g., including cracks in concrete [13] or bolt loosening detection [14, 15]).

Using a high-frequency excitation, impedance-based techniques allow for catching incipient defects in local-damage areas. The impedance-based method has main advantages, such as being sensitive to minor structural damages or easily applying for various structure forms, and interpreting data.

Despite recent attempts to apply impedance-based techniques for force estimations in PSC structures [12, 16, 17], previous studies have focused on mono-strand tendon anchorage [18] or steel-anchorage structures [12, 19-20]. There exists a need to implement the PZT interface technique for strand breakage detection in a concrete anchorage of PSC structures.

This paper presents the PZT interface technique for monitoring strand breakage in a prestressed concrete anchorage zone. At first, the fundamental of the PZT interface for impedance monitoring is reviewed. Then, a FE analysis of a concrete anchorage equipped with PZT interfaces is analyzed to obtain impedance signatures. For a series of strand breakage events, variations in impedance responses of the PZT array are quantified using the RMSD index to localized damaged strands.

2. Impedance-based strand breakage identification in the anchorage zone

2.1. PZT impedance technique for impedance monitoring

The concept of the PZT interface for impedance monitoring was proposed and verified by Huynh and Kim (2014) [10]. For the PZT interface technique, it can acquire impedance responses sensitive to structural properties with known frequency ranges (< 100 kHz). To make the PZT interface feasible for impedance measurement, the PZT and interface's mechanical specifications (e.g., geometrical and material properties) should be appropriately analyzed to determine a preferred measured frequency range.

As shown in Fig. 1, the PZT interface technique is utilized to monitor impedance responses of a prestressed tendon anchorage, which consists of an anchor block, a post-tensioning strand, and a bearing plate. As prestress force P is varied, the contact stiffness

between the bearing plate and the host structure is also changed, leading to local changes in the dynamic characteristics of the tendon anchorage. In the technique, the surface-mounted PZT patch acquires impedance responses from coupled interactions between the PZT interface and the target structure.

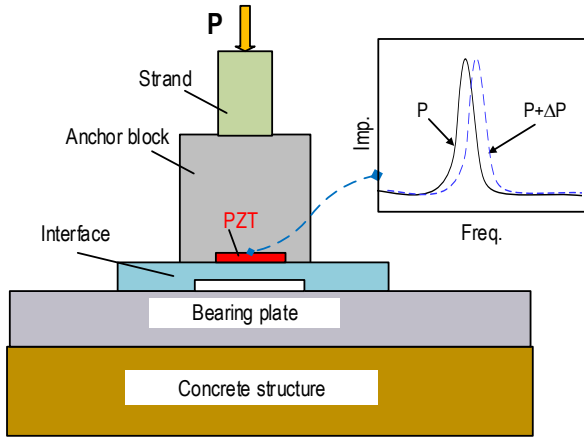


Fig. 1 Impedance monitoring concept for tendon anchorage

The ratio between the input voltage and the output current is defined as the electromechanical (EM) impedance of the system $Z(\omega)$, in which the structural impedances of the PZT sensor $Z_a(\omega)$ and the monitored structure $Z_s(\omega)$ are coupled together [21] as follows:

$$Z(\omega) = \left\{ i\omega \frac{w_a l_a}{t_a} \left[\hat{\epsilon}_{33}^T - \frac{1}{Z_a(\omega)/Z_s(\omega) + 1} d_{31}^2 \hat{Y}_{11}^E \right] \right\}^{-1} \quad (1)$$

where $\hat{Y}_{11}^E = (1+i\eta)Y_{11}^E$ is the complex Young's modulus of the PZT patch at zero electric field; $\hat{\epsilon}_{33}^T = (1-i\delta)\epsilon_{33}^T$ is the complex dielectric constant at zero stress; d_{31} is the piezoelectric coupling constant in the 1 direction at zero stress; ω is the forcing excitation frequency; $Z_a(\omega)$ is structural mechanical impedance of the PZT sensor; and w_a , l_a , and t_a are the width, length, and thickness of the PZT patch, respectively. The parameters η and δ are structural damping loss factor and dielectric loss factor of piezoelectric material, respectively.

From Eq. (1), it is obvious that $Z_s(\omega)$ structural mechanical impedance contains both structural properties of the interface and the monitored structure. Once the mechanical and electrical material properties of the PZT sensor are constants, the changes in structural properties (damage or temperature fluctuation) can be represented by the change in the EM impedance. It is noted that Equation (1) was established based on the assumption that the effects of temperature variations on piezoelectric material properties were ignored.

2.2. Statistical damage index for quantifying impedance features

It is common to use a statistical damage metric index for quantifying variations in impedance responses. The RMSD (root-mean-square-deviation) index computed changes in impedance signatures after and before damage [21] as follows:

$$RMSD = \sqrt{\frac{\sum_{j=1}^N [Z^*(\omega_j) - Z(\omega_j)]^2}{\sum_{j=1}^N [Z(\omega_j)]^2}} \quad (2)$$

where $Z(\omega_j)$ and $Z^*(\omega_j)$ are the real part of impedance signals measured in the intact, and the damage cases of the j^{th} frequency, and N symbolizes total frequency points in the sweeping frequency range.

3. Finite element model of prestressed anchorage zone with PZT interfaces

3.1. Description of target concrete anchorage

A lab-scale concrete anchorage was designed to support the 9-strand anchorage, as shown in Fig. 2 [22]. The concrete block had a size of 460×460×500 mm. A circular hole (ϕ 110 mm) was placed at the center of the concrete block for passing prestressing strands (see Fig. 2b). Reinforcement for the concrete was designed as follows: (1) orthogonal stirrups 8D10, $l = 1.76$ m; (2) orthogonal stirrups 7D10, $l = 1.28$ m; (3) a spiral D10, $l = 4.89$ m; and (4)

16D10, $l = 0.82$ m (reinforcing frame). The material properties of the concrete anchorage components are listed in Table 1.

The multi-strand anchorage consists of a 9-strand anchor head with wedges and a bearing plate. The bearing plate had the sizes of $200 \times 200 \times 35$ mm. The geometries of the anchor head were 70 mm in height and 190 mm in diameter. To simplify the FE model and reduce computation cost, steel rebar in the concrete block was converted to the Young modulus of the concrete [16].

As depicted in Fig. 3, the FE model of the multi-strand concrete anchorage equipped with the hoop-type PZT interfaces was conducted using Comsol Multiphysics. The FE model consists of an anchor head with wedges, a bearing plate, and a concrete block. Each outer strand is covered by a PZT interface, and the geometries of the interface were selected as follows: $H_{int} \times L_b \times T_b = 23 \times 18 \times 3.5$ mm, $H_{int} \times L_f \times T_f = 23 \times 24 \times 1.4$ mm, and $H_p \times L_p \times T_p =$

$15 \times 15 \times 0.51$ mm (for PZT sensor), as seen details in [19]. In this analysis, the PZT interfaces were placed at the near-bottom anchor head, as seen in Fig. 3b.

The complete meshed model consists of 21576 elements using three-dimensional elastic elements. Specifically, there were 200 elements for the PZT patches (PZTs 1-8), 872 elements for the bonding layers, 1320 elements for the eight interfaces, 720 elements for the wedges, 10998 elements for the anchor head and bearing plate, and 7466 elements for the concrete block. Hexahedron elements were used for the PZTs, the interface body, and the wedges. Meanwhile, tetrahedron elements were used for the bearing plate and the anchor head. The thickness of bonding layers (between PZT-interface and interface-anchor head) was selected as 0.1 mm. For the boundary conditions, the bottom surface of the concrete block was assigned as a fixed boundary.

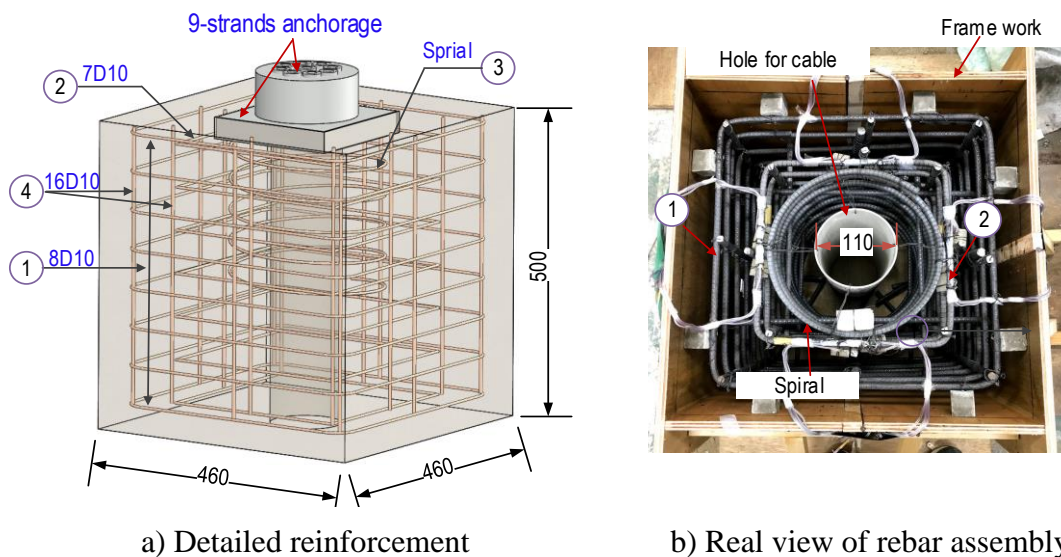


Fig. 2 Design geometry and reinforcement for concrete anchorage

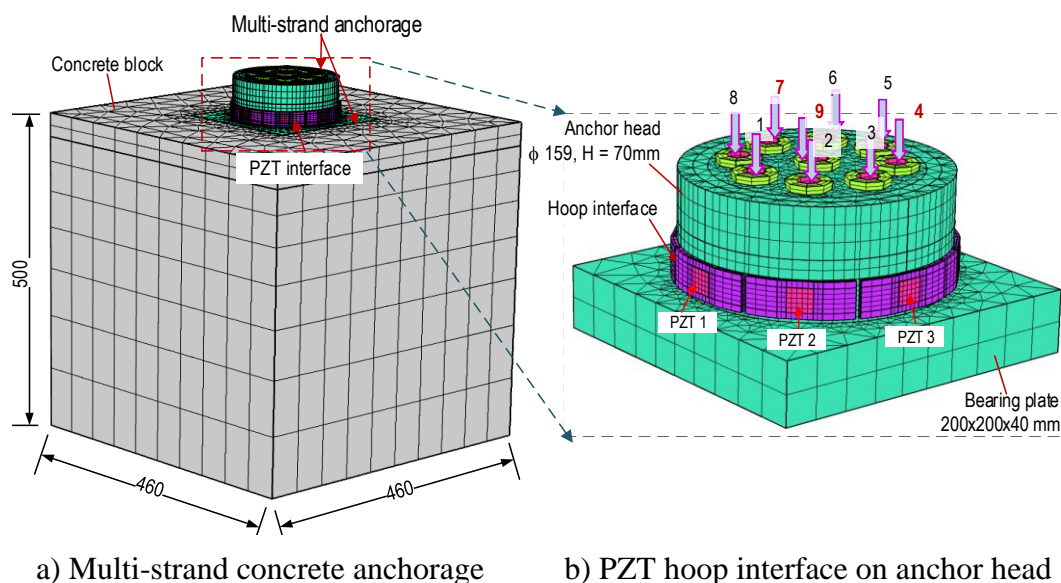


Fig. 3 FE model of concrete anchorage embedded with hoop-type PZT interfaces

Table 1. Material properties of reinforced concrete anchorage

Parameters	Anchorage components	Pure concrete	Rebar
Young's modulus (GPa)	200	24.4	200
Poisson's ratio	0.33	0.2	0.33
Mass density (kg/m ³)	7850	2400	7850
Compressive strength (MPa)	460	23.3	460

3.2. Simulation of strand breakage cases

Four simulation scenarios (PS1-PS4) were conducted in the FE model. In the intact case (PS1), each of the nine wedges (Wedges 1-9) was applied by a force of 140 kN in PS1 to simulate an intact case. In the first damage case (PS2), the prestress force of Strand 4 was assigned as zero, and the force in other strands was kept at 140 kN to simulate the breakage of Strand 4. In the second damage case (PS3), the prestress force of Strands 4 and 7 was removed in PS3 to simulate the breakage of Strands 4&7. In the last damage case (PS4), the prestress force of Strand 4, 7, and 9 were removed to simulate the triple damage strands (i.e., Strands 4, 7&9).

The impedance responses of PZTs 1-8 were acquired in the range 5-35 kHz by applying a

harmonic voltage of 1V on the top surface of the PZT sensor while the bottom surface was assigned the ground electrode.

4. Strand breakage localization in concrete anchorage zone using impedance features

4.1. Numerical impedance responses of hoop-type PZT interfaces

As shown in Fig. 4, impedance signatures of PZT 1 were plotted in the frequency range 5–35 kHz under the intact and three damage cases (PS1-4). Two resonant frequency ranges include 10.4–11 kHz (Peak 1) and 26.5–28 kHz (Peak 2).

As shown in Fig. 5, the impedance signatures of PZT sensors were zoomed for Peaks 1-2. Peak 1's impedance signatures (10.4-11 kHz) were varied under the strand

breakage cases, while Peak 2's impedance signatures (26.5-28 kHz) were almost unchanged. Specifically, the impedance responses of PZTs 4&7 had more variations than those of other PZTs (e.g., PZT 3 in Fig.

5a). Since the PZTs 4 and 7 were placed close to the damaged Strands 4 and 7, thereby resulting in higher sensitivity of impedance responses.

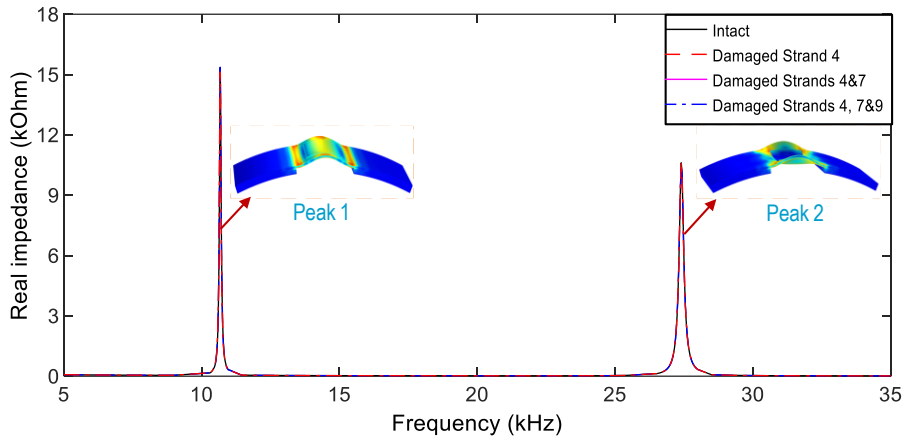
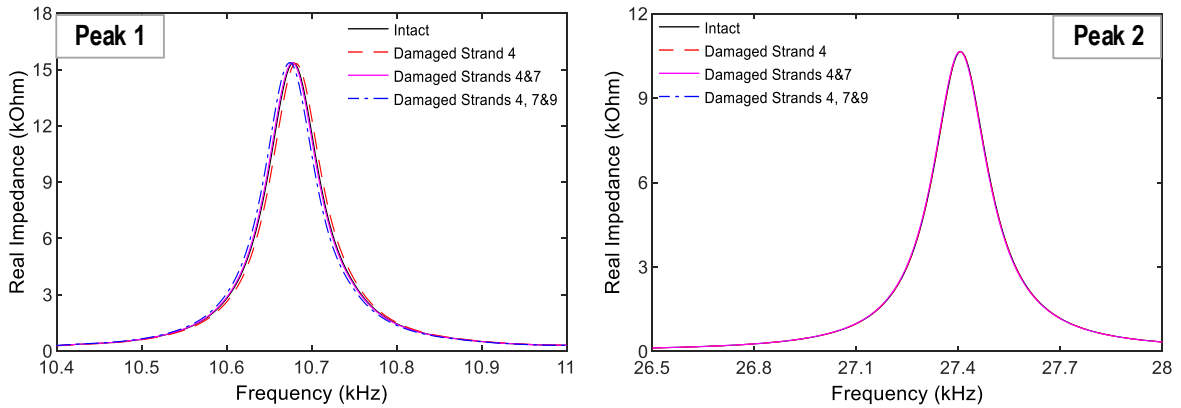
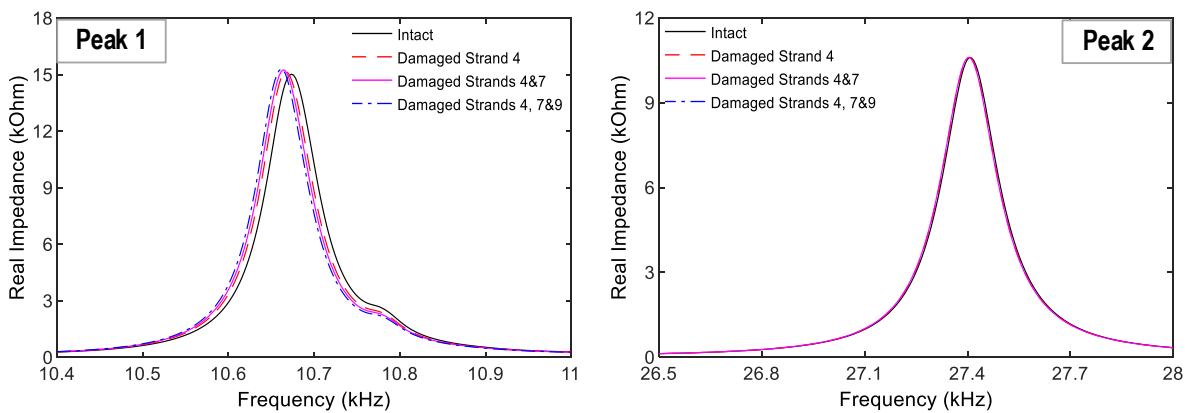


Fig. 4 PZT 1's impedance responses in the range 5-35 kHz under strand breakage cases



a) PZT 3



b) PZT 4

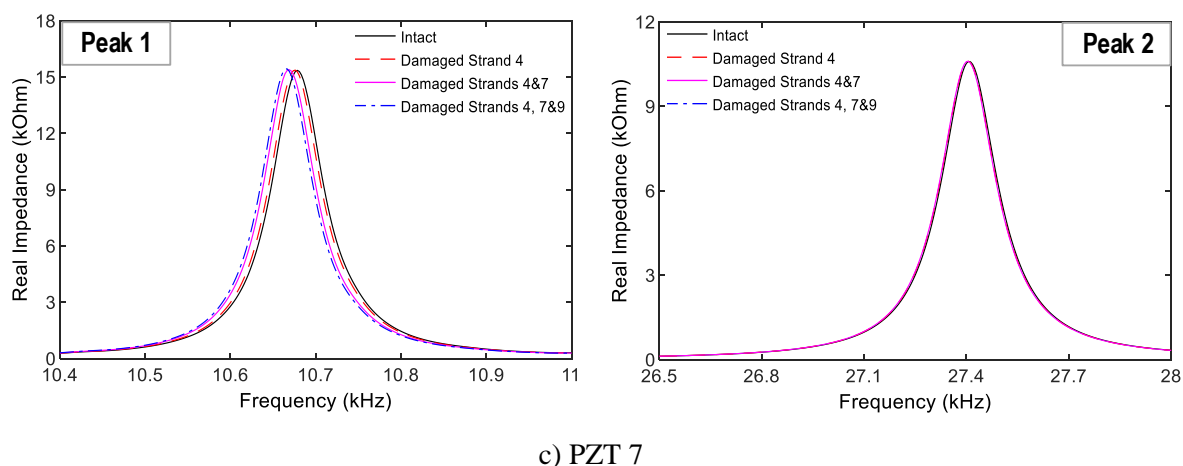


Fig. 5 Numerical impedance responses of PZT sensors under strand breakage cases

Notably, Peak 1's impedance signals of PZTs 4 and 7 were shifted to the left. Meanwhile, the impedance responses of PZT 3 were slightly rightward shifted under breakage of Strand 4, but it was leftward shifted under breakage of Strands 4, 7, and 9. It revealed that multiple damaged strands caused different effects on stress variations on the anchorage obtained via the PZT interface technique.

4.2. Linear tomography analysis of damage index for strand breakage localization

To localize damaged strands, the linear tomography of the RMSD indices was constructed over the cross-section of the anchor head. Due to Peak 1's impedance signatures being more sensitive to strand breakage, Peak 1's impedance (10.4–11 kHz) was used for the computation, as shown in Fig. 6.

For the first damage case (PS1), Fig. 6a shows the RMSD linear tomography result for the damaged Strand 4. The RMSD magnitude at Strand 4 (9.7%) was the most significant value among Strands 1-8. It indicated that the damage of Strand 4 was successfully localized.

For the second damage case (PS2), Fig. 6b shows the RMSD linear tomography result for the damage of Strands 4 and 7. The RMSD magnitudes at Strand 4 (14.2%) and Strand 7 (14.6%) were more significant than those at other strands. Specifically, the RMSD magnitudes at Strands 4 and 7 were about twice times larger than those at Strands 5&6 (6.2%) and about five times larger than that of Strand 1 (3.2%). It indicated that the damage of Strands 4 and 7 was successfully localized.

For the last damage case (PS3), Fig. 6c shows the RMSD linear tomography result for the damage of Strands 4, 7, and 9. The RMSD magnitudes at Strand 7 (i.e., 19.5%), and Strand 4 (i.e., 18.7%) were the first and second-largest values. The result suggested that the damage of two outer Strands 4, and 7 was well indicated. The RMSD indices at Strands 5-6 were ignorable (about 1.8%). Meanwhile, the RMSD indices were significant at the other strands (Strands 1-3 and 8). The result suggested that the breakage of Strand 9 was not well detected.

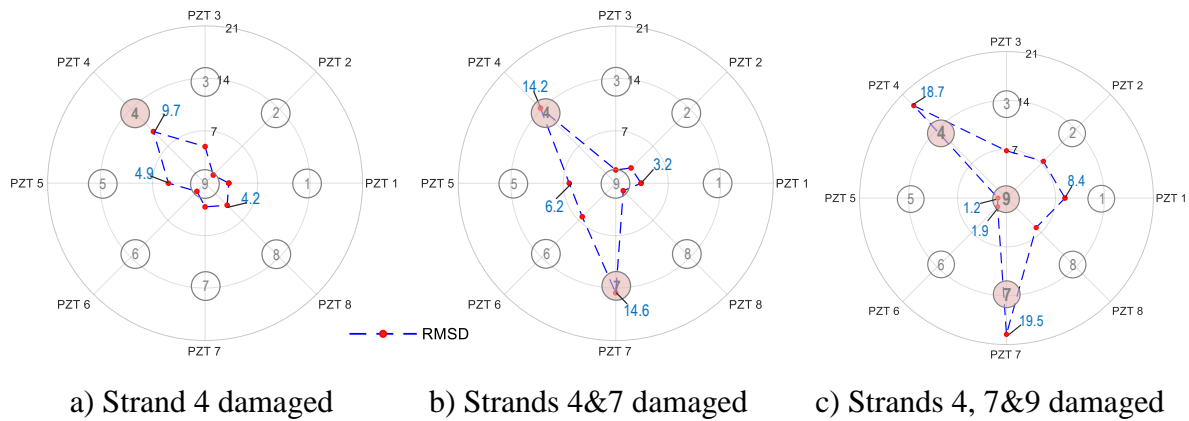


Fig. 6 Numerical linear tomography of RMSD indices (%) using Peak 1's impedance

5. Concluding remarks

This paper presented the implementation of the PZT interface technique for monitoring strand breakage in a prestressed concrete anchorage zone. At first, the fundamental of the PZT interface for impedance monitoring was briefly introduced. Second, the FE analysis of the nine-strand concrete anchorage equipped with the array of PZT interfaces was analyzed to obtain impedance signatures under a series of strand breakage events. Last, the variations in impedance responses of the PZT array are quantified using RMSD, and the linear tomography analysis of impedance's RMSD indices was utilized to localize damage strands.

From the analysis, it can be concluded that the PZT interface technique was successfully employed to monitor the health condition of the PSC structure; the locations of single and double outer damaged strands were successfully identified; and the location of a center damage strand was not clearly determined in the multiple damage case.

References

- [1] Zhu. Y.P., *et al.* (2022). Nonlinear output frequency response functions: A new evaluation approach and applications to railway and manufacturing systems' condition monitoring, *Mechanical Systems and Signal Processing*, Vol. 163.
- [2] Goldsberry. B. (2013). Post-tensioning best practice update and new directions for post-tensioned structures.
- [3] Mehrabi. A.B., *et al.* (2010). Evaluation, rehabilitation planning, and stay-cable replacement design for the hale boggs bridge in Luling, Louisiana, *Journal of Bridge Engineering*, Vol. 15 (4), pp. 364-372.
- [4] Hiba. A.J., and Glisic. B. (2018). Monitoring of long-term prestress losses in prestressed concrete structures using fiber optic sensors, *Structural Health Monitoring*, Vol. 18 (1), pp. 254-269.
- [5] James. G., *et al.* (2018). *Genoa bridge collapse: the road to tragedy*.
- [6] Ho. D.D., *et al.* (2012), Prestress-force estimation in PSC girder using modal parameters and system identification, *Advances in Structural Engineering*, Vol. 15 (6), pp. 997-1012.
- [7] Huynh. T.C., and Kim. J.T. (2017). Quantification of temperature effect on impedance monitoring via PZT interface for prestressed tendon anchorage, *Smart Materials and Structures*, Vol. 26 (12), pp. 1-19.
- [8] Yang. M., *et al.* (2020). Refined calculation of time-dependent prestress losses in prestressed concrete girders, *Structure and Infrastructure Engineering*, Vol. 16 (10), pp. 1430-1446.
- [9] Kim. J.T., *et al.* (2010). Hybrid health monitoring of prestressed concrete girder bridges by sequential vibration-impedance approaches, *Engineering Structures*, Vol. 32 (1), pp. 115-128.
- [10] Huynh. T.C., and Kim. J.T. (2014). Impedance-based cable force monitoring in tendon-anchorage using portable PZT-interface technique, *Mathematical Problems in Engineering*, Vol. 2014, pp. 1-11.
- [11] Dang. N.L., *et al.* (2019). Local strand-breakage detection in multi-strand anchorage system using an impedance-based stress monitoring method-feasibility study. *Sensors (Basel)*, Vol. 19 (5).

- [12] Min. J., *et al.* (2016). An electromechanical impedance-based method for tensile force estimation and damage diagnosis of post-tensioning systems, *Smart Structures and Systems*, Vol. 17 (1), pp. 107-122.
- [13] Ai. D., *et al.* (2019). Numerical and experimental investigation of flexural performance on pre-stressed concrete structures using electromechanical admittance, *Mechanical Systems and Signal Processing*, Vol. 128, pp. 244-265.
- [14] Wang. F., *et al.* (2018). A novel fractal contact-electromechanical impedance model for quantitative monitoring of bolted joint looseness, *IEEE Access*, Vol. 6, pp. 40212-40220.
- [15] Huynh. T.C., *et al.* (2018). Preload monitoring in bolted connection using piezoelectric-based smart interface, *Sensors (Basel)*, Vol. 18 (9).
- [16] Dang. N.L., *et al.* (2021). Piezoelectric skin sensor for electromechanical impedance responses sensitive to concrete damage in prestressed anchorage zone, *Smart Structures and Systems*, Vol. 28 (6), pp. 761-777.
- [17] Huynh. T.C., *et al.* (2015). Local dynamic characteristics of PZT impedance interface on tendon anchorage under prestress force variation, *Smart Structures and Systems*, Vol. 15 (2), pp. 375-393.
- [18] Huynh. T.C., and Kim. J.T. (2017). Quantitative damage identification in tendon anchorage via PZT interface-based impedance monitoring technique, *Smart Structures and Systems*, Vol. 20 (2), pp. 181-195.
- [19] Dang. N.L., *et al.* (2020). Piezoelectric-based hoop-type interface for impedance monitoring of local strand breakage in prestressed multi-strand anchorage, *Structural Control and Health Monitoring*, Vol. 28 (1), pp. 1-20.
- [20] Dang. N.L. (2020). *Smart impedance monitoring technique for multi-strand anchorage in prestressed concrete structures*, Ph.D. Thesis, Department of Ocean Engineering, Pukyong National University, Korea.
- [21] Sun. F.P., *et al.* (1995). Truss structure integrity identification using PZT sensor-actuator, *Journal of Intelligent Material Systems and Structures*, Vol. 6 (1), pp. 134-139.
- [22] Pham. Q.Q., *et al.* (2021). Optimal localization of smart aggregate sensor for concrete damage monitoring in psc anchorage zone, *Sensors (Basel)*, Vol. 21 (19).